Discrete film thickness in polyacrylamide-CdS nanocomposite ultrathin films

Amarjeet Singh and M. Mukherjee
Surface Physics Division, Saha Institute of Nuclear Physics, 1/AF, Bidhannagar, Kolkata-700064, India
(Received 11 February 2004; revised manuscript received 6 July 2004; published 24 November 2004)

A nanocomposite of polyacrylamide, a water soluble polymer, and nanocrystalline CdS has been prepared using a chemical route. Transmission electron microscope observation shows that the particles are attached via the polymer coils. The reduction of viscosity for the composite, despite the increase in concentration, indicates a reduction of interchain entanglement between the composite coils. Ultrathin films were prepared from the nanocomposite and pure polyacrylamide using spin coating on a Si(100) substrate in the speed range of 500 to 5000 rpm. X-ray reflectivity studies of the pure polymer and composite films were carried out in vacuum. The thickness of the composite films varies nonmonotonically with spinning speed and is found to lie in discrete "bands" of thickness separated by "forbidden regions." The power law behavior of the thickness with the spinning speed was also found to be different for the composite films in comparison to the polymer ones. A model has been proposed in terms of discrete numbers of layers composed of CdS-attached polymer coils to explain the phenomena.

DOI: 10.1103/PhysRevE.70.051608 PACS number(s): 68.47.Pe, 61.10.Kw, 82.70.−y

I. INTRODUCTION

Studies of the structure and dynamics of ultrathin polymer and polymer nanocomposite films on a substrate are of fundamental as well as applied interest. In polymer films, the large number of molecules that are in intimate contact with the substrate surface and the confinement of the chains in one dimension lead to many interesting properties [1–5]. In the case of polymer nanocomposite systems, which are homogeneous dispersions of a nanocrystalline phase in a polymer medium, the presence of nanocrystalline particles further modifies the properties due to the introduction of a second phase and the large amount of interfacial region in these systems [6–10]. Nanometer sized CdS particles dispersed in a continuous polymer matrix have attracted much attention owing to their unique optical and electronic properties and their potential application in solar energy conversion [11–14]. The spin coating technique has been used to prepare ultrathin polymer and nanocomposite films in our study. This technique is widely used for applying thin uniform photoresist films to flat silicon substrates in the microelectronics industry. It is used for coating of color television screens, optical devices, and magnetic storage disks. There is a rich literature on the theoretical and experimental studies of spin coated photoresist and polymer films [15–22]. It is generally possible to obtain highly uniform films of any viscous fluids and the final film thickness depends mainly on two parameters—the concentration of the solution and the final spinning speed. Other parameters like the acceleration of the rotating disk and the initial volume of the solution dispensed onto the rotating disk have negligible or no effect. The final thickness of the films shows a power law dependence on the angular speed of the rotating disk. However, systematic studies of the structure of spin coated ultrathin polymer nanocomposite films, particularly with water soluble polymers, are not available in the literature. In the present study we have prepared a CdS-polyacrylamide nanocomposite through a chemical route and used it to prepare thin films in a range of thicknesses using the spin coating technique. The thickness and the internal structure of the pure polymer as well as nanocomposite films were studied using x-ray reflectivity technique. In the present article we report the following observations for the composite films unlike the polymer ones: (a) discontinuous film thickness as a function of the spinning speed of coating, (b) layering in the electron density profile as a function of depth, and (c) a different power law dependence of the thickness on the spinning speed. An attempt has been made here to explain the phenomena with a model in terms of single or multiple layers of composite polymer coils.

II. EXPERIMENTAL DETAILS

A. Sample preparation

To prepare the nanocomposite material with a CdS concentration of 5% by volume, a measured amount of cadmium acetate was dissolved in 0.2 mg/ml of polyacrylamide ($M_w > 5\times10^6$, BDH Chemicals, U.K.) solution in water. 500 ml of the above solution was kept boiling at 100 °C and H_2S gas was passes through the solution following Mukherjee *et al.* [7]. As the gas was passed, the solution started becoming yellow and within five minutes the whole solution turned yellow, ensuring that all cadmium acetate had reacted completely with H_2S to form CdS. After stopping the gas flow the solution was kept boiling for 10 min to ensure complete removal of excess H_2S from the sol. A small amount of yellow flakes was observed at the bottom of the container. The composite sol was subsequently filtered using a clean cotton cloth washed with Millipore water. During filtration some material stuck to the filter cloth that could not be recovered, resulting in some material loss. To eliminate acetic acid from the sol it was boiled for several hours. The concentration of the final sol was measured by weighing the dried mass of a measured volume of the sol and was found to be 5.6 mg/ml.

The average size of the CdS particles formed in the reaction was estimated to be 4.2 nm from the blueshift of the

absorption band edge measured by uv-visible (uv-vis) spectroscopy (Cintra 10_e, GBC) [23]. The relative viscosity of the composite sol and a 2 mg/ml polyacrylamide solution, which was used to prepare the polymer films, were estimated by measuring the efflux time through a capillary. We observed about 16 times reduction of the relative viscosity of the composite sol compared to the polymer solution. The hydrodynamic radii R_H of the polymer and the composite coils in solutions of the above mentioned concentrations were measured using dynamic light scattering (DLS-7000, Otsuka Electronics) and were found to be 1170 and 270 nm, respectively. The lower R_H value and the reduction of relative viscosity despite the increase in concentration of the composite suggest that the intercoil entanglement of the polymer chains was reduced when they were loaded with CdS particles. This is possibly due to the reduction of the amount of hydrogen bonds between the polymer chains and the surrounding water molecules. No separation of the polymer phase and the CdS nanoparticles was observed even after centrifuging the composite sol at 20 000 rpm for 20 min, which indicates that the nanosized CdS particles were sterically stabilized [24] by the polymer molecules.

The composite sol was used to prepare thin films on a Si(100) substrate using the spin coating technique with a range of rotation speeds from 500 to 5000 rpm. To make the surface suitably hydrophilic for coating of water soluble polymers, the silicon wafers were chemically treated with a mixture of ammonia solution and hydrogen peroxide ($NH_4OH:H_2O_2:H_2O=1:1:2$) at boiling temperature for 5 min before spin coating on them. During the spinning, clean and warm air (60 °C) was flowed gently over the sol using a homemade arrangement to facilitate a faster evaporation of water. Using a similar technique, films of pure polymer were also prepared for comparative studies. For preparing these films a 2 mg/ml polyacrylamide solution was used. It is to be noted that for this concentration we obtained films of similar thickness to those of the composite ones for similar spinning speeds (see Fig. 2). It is generally observed that the spin coated films, especially the ones rotated at high speed, may remain in a nonequilibrium structure. The films were kept for 30 min in a closed container with an open pot of water inside. Since the polymer was water soluble, the films absorbed water vapor and swelled and as a result released the strain to attain equilibrium structures. The films were then stored in a desiccator for drying.

B. Transmission electron microscopy

Transmission electron microscopy (TEM) (Hitachi H600 operated at 100 kV) was used to study the internal structure of the nanocomposite material in the as-prepared and the thin film forms. A drop of dilute (1 mg/ml) sol was poured on a carbon coated copper grid and was allowed to dry for observation of the as-prepared sample. The micrograph in Fig. 1(a) corresponding to this sample clearly shows a few flakelike objects with dark dots in them. The lateral dimension of the individual flakes is close to the R_g of the polymer, which suggests that the composite material is composed of CdS particles that are attached to the individual polymer coils.

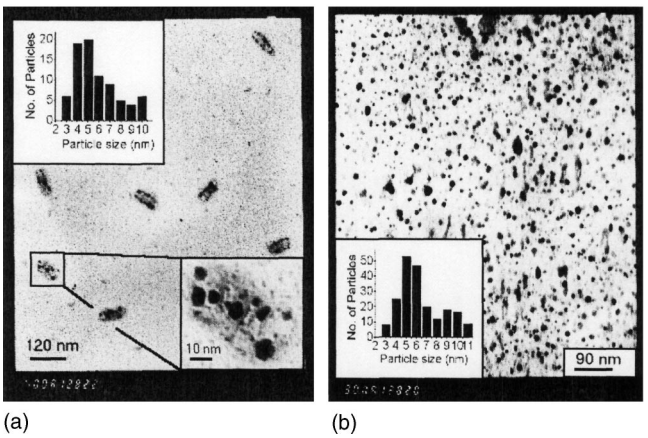

FIG. 1. (a) The micrograph obtained from as-prepared nanocomposite at 60 000 magnification. The higher magnified view of a flakelike object is shown in the inset. (b) The micrograph obtained from spin coated grid at 80 000 magnification. The black dots in the micrograph are the CdS particles. The particle size distributions are also shown in the insets of the corresponding micrographs.

One of these flakes has been shown in the inset of the figure with higher magnification, where dispersed nanocrystalline CdS particles are clearly observed in the polymer matrix. To get a true picture of the internal structure of a thin film constructed from the nanocomposite material we prepared a second grid by spin coating the composite material directly on it. An uncoated grid was mounted by a tiny drop of resin on a silicon substrate and the substrate was spin coated at 5000 rpm, following identical procedures as for the 5000 rpm film used for x-ray reflectivity experiments. In Fig. 1(b), we have shown the TEM micrograph corresponding to the spin coated grid, which is a true representation of the internal structure of a composite film coated at 5000 rpm. The figure shows dispersed CdS particles only; the polymer part is not visible here. We believe that the thin films are constructed of the interconnected flakelike objects shown in Fig. 1(a). The average interparticle separation of the CdS particles for both the micrographs was calculated for comparison with the numbers obtained from the analysis of the x-ray data (discussed later). The average separation for the first grid was 120 ± 8 Å whereas for the second grid the separation was higher due to stretching during spin coating and was observed to be 175 ± 10 Å. The particle size distributions are shown in the insets of the corresponding figures. The average particle size observed from TEM was found to be in close agreement with that observed from uv-vis measurements.

C. X-ray reflectivity

X-ray reflectivity is one of the powerful techniques to characterize thin films and interfaces. An x-ray beam falls on the film at glancing angles and is reflected at the interfaces. For x rays, the interface is defined as the separation of two media with different electron densities. A polymeric material with sufficient electron density contrast with that of the substrate (silicon) can be characterized using x-ray reflectivity.

The details of the technique can be found in Refs. [26,27].

We performed specular reflectivity (the angle of incidence equals the angle of reflection) to characterize the nanocomposite thin films. Polyacrylamide, being soluble in water, is hygroscopic, and hence the structure of dry polymer films could not be obtained in atmospheric conditions. For taking x-ray data the samples were mounted in a vacuum chamber and heated *in situ* at 70 °C for 20 min in vacuum (0.07 Torr) for annealing and drying. The films were then cooled to room temperature (26 °C) without breaking the vacuum.

The x-ray specular reflectivity scans were taken at room temperature in vacuum using Cu $K\alpha 1$ monochromated radiation from a rotating anode x-ray source (Enraf Nonius FR591). The data for all the films with good statistics were collected up to the incident angle of 3.5° and were analyzed using the Parratt formalism [25] modified to include interfacial roughness [26,27]. For the analysis of the data for nanocomposite films, the input electron density profiles were divided into several boxes of equal thickness and interfacial roughnesses of 2–5 Å were used to account for gradual changes of electron density due to the presence of the dispersed phase. The top and the substrate roughness along with the electron densities of all the layers corresponding to the films were varied during the fitting process. For pure polymers a single electron density for the entire film with a lower density layer between the film and the substrate having suitable top and substrate roughness were sufficient to obtain very good fits. The lower density values above the substrate observed for both polymer and composite films indicate that the density of the anchoring chains was lower than the bulk density of the films, with similar values in both cases. The observed thickness of all the films ranges between 60 and 370 Å, which is much less than the radius of gyration R_g of the polymer (~100 nm).

III. RESULTS AND DISCUSSION

The analysis of the x-ray reflectivity data for the composite films shows that the film thickness does not change monotonically as a function of spinning speed. Within the limit of our experiments we have observed three discrete "bands" of film thickness separated by two "forbidden regions." The thickness of the polymer films, on the other hand, continuously changes with the speed as expected. In Fig. 2 we have compared the thickness of the polymer films with those of the composite ones. The thickness of the polymer films shows a continuous change as a function of the speed of preparation. On the other hand, the thickness of the composite films was found to occur within discrete thickness regions of 106–155 Å, 227–251 Å, and 310–362 Å. It can be clearly seen from Fig. 2 that the thicknesses of the composite films at most of the speeds were similar to or higher than those of the polymer films, although the concentration of the composite sol was about three times higher than the pure polymer solution. The discreteness and the departure of the predicted dependence of the film thickness on the initial concentration of the solution for the spin coated films [20] indicate that the internal structure of the composite films may be different from that of the polymer films.

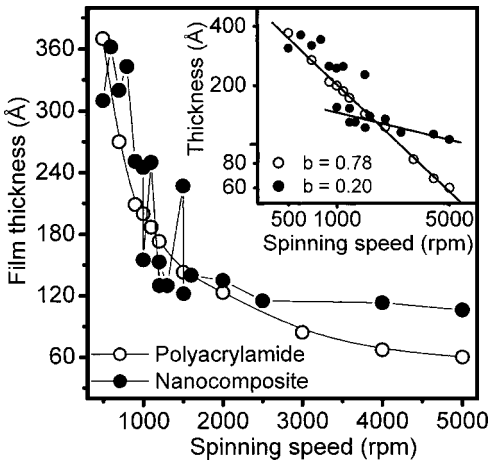

FIG. 2. Thickness of the polyacrylamide (open symbols) and nanocomposite films (solid symbols) as a function of the spinning speed. Lines connecting the symbols are guides to the eyes. The inset shows the logarithmic plot of the same data. The slope of the straight line fits in the inset represents the power law behavior of the data (parameter b). The uncertainties in the thickness values are smaller than the size of the symbols.

Another notable feature of the thickness values for the composite films was the fluctuations of these values close to the transition region between the "allowed bands," as indicated in the figure by the line connecting the data points. This suggests that the thickness of the films may have a strong dependence on minute fluctuations of parameters like spinning speed, roughness of the substrate, or the temperature of the warm air that was circulated during their preparation. To test the influence of these factors on the film thickness we prepared some of the samples on a second substrate without changing any preparation parameter. The thickness of some of these films was found to change significantly. At least in two cases, for 1000 and 1500 rpm, the film thickness jumped from one band to another as can be seen in the figure. This clearly indicates that the thickness of the composite films was strongly influenced by the fluctuations of these preparation parameters, although it was not possible to identify any systematic pattern. The sudden change of the film thickness by about 100 Å at certain speeds indicates that the films might be constructed by the stacking of layers of around 100 Å thick and loss of such layers gives rise to a discrete change in the film thickness. As the radial velocity of the molecules during spin coating increases quadratically with the height from the substrate [15], one can understand that the topmost layer encounters the highest centrifugal force and as a result snapping off of the layer occurs when the centrifugal force exceeds the interlayer friction.

In the inset of Fig. 2 we have shown the logarithmic plot of the same data shown in Fig. 2 along with the straight line fits. It is well documented that spin coated films follow a power law dependence between the film thickness z and the spinning speed ω given by $z \propto \omega^{-b}$. The majority of the experimental and theoretical investigations [15–22] report a value of 0.5 for b. For the polymer films we obtained a value of $b=0.78$; a similar value 0.8 was earlier observed for spin coated high viscosity polyimide films [28]. Higher values of

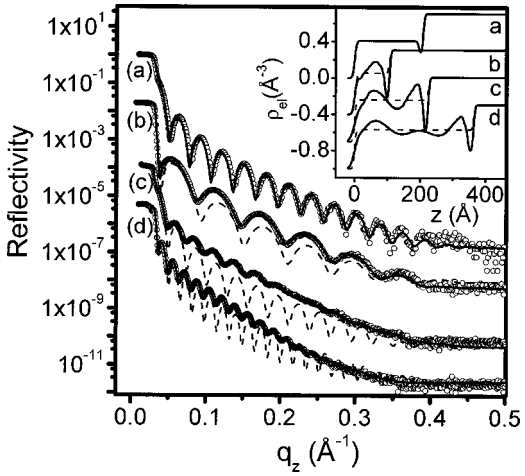

FIG. 3. X-ray reflectivity data (symbol) along with the fittings (solid line) for (a) polyacrylamide film prepared at 700 rpm (208 Å) and (b)–(d) nanocomposite films prepared with the speeds (b) 5000 rpm (106 Å), (c) 1500 rpm (224 Å), (d) 500 rpm (363 Å). The inset shows the electron density profiles for the corresponding films as obtained from the reflectivity data. All the reflectivity and the electron density profiles for the composite films (b)–(d) have been shifted suitably for clarity. The simulated reflectivity curves (dashed lines) for the flat electron density profiles (inset) are also shown for comparison.

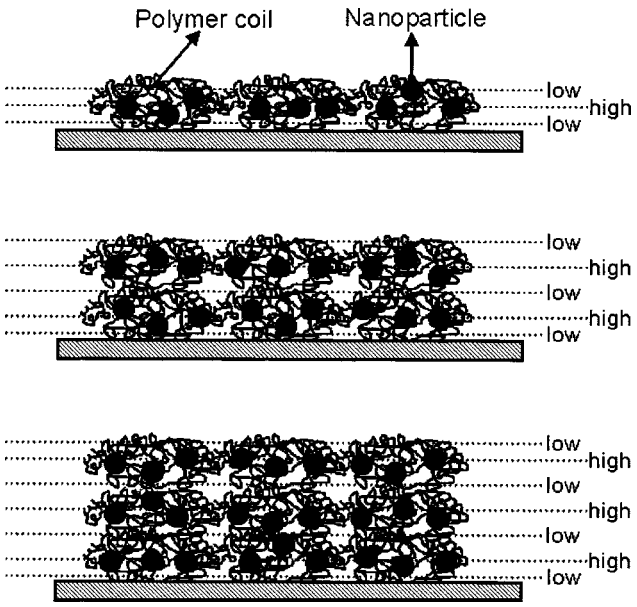

FIG. 4. The schematic model for the nanocomposite films. The thin curly lines and the black solid circles represent the polymer chains and the CdS particles, respectively. (Top) the thinnest films are shown to be formed by a layer of laterally entangled individual coils. (Middle) the intermediate thickness (curve *c* in Fig. 3) and (Bottom) high thickness (curve *d* in Fig. 3) films are shown to be constructed by stacking of additional similar layers of which the thinnest film is formed. The dotted lines are drawn to represent alternating low and high electron density regions observed from the three representative electron density profiles discussed in the text.

b were also predicted by Yonkoski and Soana [21] in terms of shorter spinning times. In the case of the nanocomposite films the data were discontinuous; hence the fitting was done with the region of thickness lying between 106 and 155 Å where the thickness change was continuous. We find $b=0.2$ which is much lower in magnitude compared to that of polymer films. This indicates that these films were less compressible than those made of pure polymers. Although lower values of *b* for spin coated films for lower initial polymer concentrations were experimentally observed [17,18], no theoretical prediction supports lower *b* values so far. The available theories for the spin coated films are developed for continuous Newtonian or non-Newtonian fluids but the composite sol behaves like a discontinuous system due to the presence of discrete structures, as can be observed by TEM [Fig. 1(a)]. In the present case the lowering of entanglement (lower viscosity) as a result of structural modification of the polymer coils due to the attached CdS particles makes these systems behave like fluids with spatial variation of mechanical properties, and the theoretical predictions for the continuous fluids may not be valid here.

In Fig. 3 we have shown the x-ray reflectivity data for three representative composite films from the three different thickness bands mentioned above along with typical data for a polymer film with corresponding fittings for comparison. The inset of the figure shows the electron density profiles for the films as observed from the analysis of the reflectivity data. A comparison between the reflectivity data for the polymer and composite films shows the smearing of the oscillation amplitudes for the composite films. This was also observed earlier as a characteristic feature in similar systems [11] due to internal density fluctuations in them. Comparison of the results in the inset of Fig. 3 shows that the electron density for the polymer film was uniform throughout the film with a lowering of the same close to the substrate, whereas the profiles show variation of electron density in the composite films as a function of depth. Single or multiple hump structures in the density profiles were observed for the composite films with the size of the humps larger than the average size of the CdS particles. To estimate the reasonableness of the humps in the electron density profiles we have simulated the reflectivity curves using a flat average electron density for the composite films. These profiles are also shown in Fig. 3 for comparison. The difference of the simulated profiles from the experimental data indicates that the variations in the electron density are real and suggests that the films were constructed of single or multiple layers of higher density material separated by lower density interfaces. A single hump can be clearly observed in the density profile for the thinnest film (inset curve *b*). The hump at around halfway between the top surface and the substrate with an electron density value higher than the polymer indicates that the film may be constructed by lateral placement of the entangled composite coils. The lower electron density close to the substrate and the top surface of the films suggests that the coils are likely to be polymer molecules in which CdS nanoparticles were encapsulated. In Fig. 4 we have shown the schematic model of the nanocomposite films on the basis of the observations described above. The schematic shows that the single layer film is constructed by the lateral placement of the CdS embedded coils and the higher thickness films are formed by the addition of an integral number of such layers.

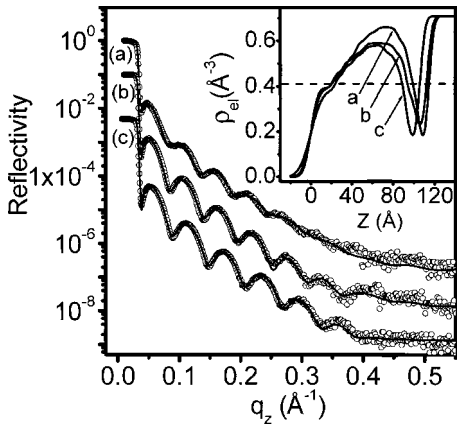

FIG. 5. X-ray reflectivity data (symbols) along with the fittings (solid line) for the nanocomposite films prepared with three highest spinning speeds (a) 2500 rpm (115 Å), (b) 4000 rpm (113 Å), and (c) 5000 rpm (106 Å). The inset shows the electron density profiles for the corresponding films as obtained from the reflectivity data and the dashed line represents the bulk polymer density. The reflectivity profiles (b) and (c) have been shifted suitably for clarity.

The alternate low and high density regions observed in the electron density (inset curves $b-d$) can be explained in terms of interfaces between the layers and the interior of the layers, respectively, as indicated by dotted lines in Fig. 4.

In Fig. 5 we show the reflectivity data along with the fitted profiles corresponding to the films prepared with the three highest spinning speeds. The inset of the figure shows the electron density profiles obtained from the analysis of the reflectivity data. The thickness and the average electron density of the films were found to decrease with increasing spinning speed, as expected. The quality of the reflectivity data was found to improve for films prepared with higher speeds. This was reflected by the larger amplitude of oscillations up to larger incident angle for the films prepared at higher speeds. In other words, the quality of the films has improved due to reduction of the top roughness and internal electron density fluctuation as a result of stretching of the composite coils, ruling out any possibility of dewetting as a cause of density reduction. Considering the assumption that the hump regions in the electron density profiles appeared due to the presence of CdS particles, we have estimated the interparticle separation of the CdS particles for these films. Using the known values of the electron densities ρ_e^{CdS} and ρ_e^{poly} for CdS and polymer and the observed electron density for the composite ρ_e^{comp} one can calculate the electronic fraction f for the CdS phase in a composite film using $\rho_e^{\mathrm{CdS}} f + \rho_e^{\mathrm{poly}}(1-f) = \rho_e^{\mathrm{comp}}$. Here the average value of ρ_e^{comp} was calculated by dividing the area under a particular density profile by its thickness. For this purpose we have considered only that portion of the thickness for which the electron density was higher than that of the pure polymer (0.42 Å^{-3}, shown in the inset of the figure by a dotted line). Knowing the mass densities ρ_m^{CdS} and ρ_m^{poly} for CdS and the polymer and the known value of f, one can calculate the weighted mass density of the composite ρ_m^{comp} using $(\rho_m^{\mathrm{CdS}}/\rho_e^{\mathrm{CdS}}) f + (\rho_m^{\mathrm{poly}}/\rho_e^{\mathrm{poly}})(1-f) = \rho_m^{\mathrm{comp}}/\rho_e^{\mathrm{comp}}$. From this mass density of the composite, the mass fraction of CdS particles was calculated. Considering the volume under unit surface area of the film, we calculated the mass contained in this volume. Dividing the total mass corresponding to the CdS particles by the mass of a single particle one can get the number of particles for the entire volume considered. From the calculated number of CdS particles homogeneously distributed in a known volume we obtained the interparticle separation of 115, 132, and 140 Å for the films prepared at 2500, 4000, and 5000 rpm, respectively. A similar trend for the change of interparticle separation was also observed from TEM measurements. The range of interparticle separations obtained from TEM matches quite well with the above numbers. For the as-prepared sample there was no stretching; hence, the interparticle separation was minimum, and for the thin film sample higher separation was observed due to stretching. The increase of interparticle separation with stretching of the films further reveals the fact that the CdS particles are strongly attached to the polymer coils.

IV. CONCLUSION

In conclusion, ultrathin films from a chemically synthesized CdS-polyacrylamide nanocomposite sol were prepared using spin coating at different speeds on a silicon wafer. Polyacrylamide films of similar thickness were also prepared for comparison. The x-ray reflectivity technique has been used to study the structure of the films. The analysis of the data shows that, unlike polymer films, the thickness of the composite films does not change monotonically with spinning speed of their preparation and their thickness lies within some discrete "bands" separated by "forbidden regions." The power law behavior of the thickness of the composite films with spinning speed was found to be widely different from that of the pure polymer. We believe there is a change in the hydrodynamic behavior of the composite sol compared to the polymer solution due to the CdS particles attached to the polymer chains. This is also reflected by the drastic reduction of the relative viscosity despite the threefold increase in the concentration. We have shown by TEM measurements that, during the preparation of nanomaterials within the polymer matrix through the chemical route, CdS particles were attached to the individual polymer molecules and as a result the interchain entanglement between the polymer molecules was reduced. We propose that the ultrathin films that were prepared form the composite sol were constructed in the form of single or multiple stacks of these composite units.

ACKNOWLEDGMENT

The authors thankfully acknowledge Pulak Ray for his assistance with TEM measurements.

[1] E. K. Lin, R. Kolb, S. K. Satija, and W. L. Wu, Macromolecules **32**, 3753 (1999).
[2] J. Kraus, P. Muller-Buschbaum, T. Kuhlmann, D. W. Schubert, and M. Stamm, Europhys. Lett. **49**, 210 (2000).
[3] M. Mukherjee, M. Bhattacharya, M. K. Sanyal, Th. Geue, J. Grenzer, and U. Pietsch, Phys. Rev. E **66**, 061801 (2002).
[4] A. Singh and M. Mukherjee, Macromolecules **36**, 8728 (2003), and references therein.
[5] Y. Tang, T. J. Su, J. Armstrong, J. R. Lu, A. L. Lewis, T. A. Vick, P. W. Startford, R. K. Heenan, and J. Penfold, Macromolecules **36**, 8440 (2003).
[6] J. U. Kim and Ben O'Shaughnessy Phys. Rev. Lett. **89**, 238301 (2002).
[7] M. Mukherjee, A. Dutta, and D. Chakravorty, Appl. Phys. Lett. **64**, 1159 (1994).
[8] D. H. Cole, K. R. Shull, L. E. Rehn, and P. Baldo, Phys. Rev. Lett. **78**, 5006 (1997).
[9] M. Mukherjee, D. Chakravorty, and P. M. G. Nambissan, Phys. Rev. B **57**, 848 (1998).
[10] P. Mustarelli, C. Capiglia, E. Quartarone, C. Tomasi, P. Ferloni, and L. Linati, Phys. Rev. B **60**, 7228 (1999).
[11] M. Mukherjee, N. Deshmukh, and S. K. Kulkarni, Appl. Surf. Sci. **218**, 323 (2003).
[12] S. W. Yeh, and K. H. Wei, Macromolecules **36**, 7907 (2003).
[13] Z. P. Qiao, Y. Xie, G. Li, Y. J. Zhu, and Y. T. Qian, J. Mater. Sci. **35**, 285 (2000).
[14] M. Chen, Y. Xie, Z. P. Qiao, Y. J. Zhu, and Y. T. Qian, J. Mater. Chem. **10**, 329 (2000).
[15] A. G. Emslie, F. T. Bonner, and L. G. Peck, J. Appl. Phys. **29**, 858 (1958).
[16] A. Acrivos, M. J. Shah, and E. E. Petersen, J. Appl. Phys. **31**, 963 (1960).
[17] D. Meyerhofer, J. Appl. Phys. **49**, 3993 (1978).
[18] W. W. Flack, D. S. Soong, A. T. Bell, and D. W. Hess, J. Appl. Phys. **56**, 1199 (1984).
[19] M. Yanagisawa, J. Appl. Phys. **61**, 1034 (1987).
[20] C. J. Lawrence, Phys. Fluids **31**, 2786 (1988).
[21] R. K. Yonkoski and D. S. Soana, J. Appl. Phys. **72**, 725 (1992).
[22] S. K. Wilson, R. Hunt, and B. R. Duffy, J. Fluid Mech. **413**, 65 (2000).
[23] Y. Wang and N. Herron, Phys. Rev. B **42**, 7253 (1990).
[24] *Soft Matter Physics*, edited by M. Daoud and C. E. Williams (Springer, Berlin, 1999).
[25] L. G. Parratt, Phys. Rev. **95**, 359 (1954).
[26] T. P. Russel, *Materials Science Reports* (Elsevier North-Holland, Amsterdam, 1990), Vol. 5.
[27] Jean Dailland and Alain Gibaud, *X-Ray and Neutron Reflectivity: Principles and Applications*, (Springer, Berlin, 1999).
[28] W. J. Daughton and F. L. Givens, J. Electrochem. Soc. **129**, 173 (1982).